World Journal of Engineering Research
Print ISSN: 2959-9865
Online ISSN: 2959-9873
DOI: https://doi.org/10.61784/wjer3044

A DOUBLE LIQUID STORAGE LOOP HEAT PIPE BASED ON SLIDING SLEEVE REGULATION

XuanNing Liang, Jing Zhang, ZhengJie Liu, Feng Qu, WenXian Kuang, ShengNan Yan, Heng Xiao*
College of Energy and Power Engineering, Xihua University, Chengdu 610039, Sichuan, China.
Corresponding Author: Heng Xiao, Email: xiaoheng@xhu.edu.cn

Abstract: To address the limitations of traditional loop heat pipe evaporators-such as uncertain operational performance under different orientation configurations, unreasonable working fluid volume in the reservoir, and thermal leakage issues—this study proposes a novel dual-reservoir loop heat pipe. Featuring an annular nozzle-coupled sleeve design, this innovative configuration enhances heat transfer efficiency during complex gravitational variations. The research investigates how varying gravitational orientations and liquid filling rates affect the heat transfer characteristics of the dual-reservoir loop. Simulation software was employed to evaluate thermal performance across different gravitational conditions and filling rates. Results demonstrate that under 65% working fluid filling rate and 40W thermal load, the phase-change liquid medium is replenished promptly. Continuous evaporation occurs on the capillary core surface without drying out, ensuring stable operation of the loop heat pipe. This design effectively meets the mission's requirements for stable thermal dissipation in complex aerospace environments.
Keywords: Loop heat pipe; Double liquid chamber; Thermal stability; Phase change heat transfer; Thin liquid film boiling

1 INTRODUCTION

With the rapid development of artificial intelligence, quantum computing, 5G communication technology and so on, the heat generated by related electronic devices per unit volume increases rapidly, and the traditional heat dissipation means can no longer meet the demand. The development of new efficient heat dissipation technology is the key to ensure the safe and stable operation of electronic devices.

Electronic devices employ various cooling methods, including air-cooling and liquid-cooling systems, with phase-change cooling demonstrating the most effective performance[1]. The Loop Heat Pipe (LHP) is a closed-loop annular heat pipe that utilizes phase change of working fluids to drive thermal circulation, offering advantages such as high heat transfer efficiency and uniform temperature distribution. As an advanced cooling technology, its gas-liquid fluid pathways enable long-distance heat transfer without external power supply, while adapting to complex installation environments. With broad application prospects in electronics cooling, aerospace, and other fields, LHP has garnered significant attention. Researchers have conducted extensive studies on LHP parameters including working fluid properties, fluid charge volume, placement angles, and evaporator structures.

Yang Chengxiang et al. developed a novel sodium-based flat evaporator high-temperature loop heat pipe (HTLHP) for hypersonic aircraft exhaust nozzle thermal protection[2], establishing its design process and conducting heat transfer limit simulation analysis. Experimental studies investigated the effects of condensation intensity, heat pipe structure, and inclination angle on startup characteristics and heat transfer performance. The findings revealed that appropriate condensation and inclination angles could resolve startup oscillation issues, achieving a minimum heat transfer resistance of 0.0368°C/W. It was emphasized that controlling heat leakage in the liquid reservoir and maintaining working fluid reflux stability were crucial for performance enhancement. Zhang Hongxing et al. designed a dual-liquid-tank ammonia-stainless steel loop heat pipe (LHP) to overcome orientation limitations during gravity field operations[3]. By precisely matching liquid tank volume with working fluid charge, they ensured continuous liquid filling in the liquid channel, avoiding challenging startup scenarios. Experimental verification demonstrated successful operation under various orientations. However, significant temperature variations occurred between orientations within the variable thermal conductivity zone (75-250W), attributed to differing cooling effects of reflux liquid overcooling in the liquid guide tubes. Niu Wenjing et al. proposed a heat pipe-fuel system-based cooling method for severe electrical actuator heating[4]. Numerical simulations revealed that when the equivalent heat transfer coefficient of heat pipes reached 7000W/(m·K), thermal management of electrical actuators was effective. Further increases in heat transfer coefficients showed limited improvement in cooling performance. Wang Dongdong et al. improved the heat dissipation performance of loop heat pipes (LHP) by optimizing evaporator sealing processes and designing a dual-capillary-core structure[5]. Experimental results showed that the maximum operational thermal load increased from 140W to 240W under welded sealing, while the dual-capillary core design effectively reduced lateral wall heat transfer, enhancing system startup and operational efficiency. Xia Yijun et al. developed a novel micro-channel loop heat pipe[6]. Through experimental and simulation studies on its heat exchange performance, it was found that the heat pipe operates stably across 30W-180W thermal loads with rapid response during variable load testing, demonstrating excellent reliability. The research also revealed that modified capillary core structures significantly increase refrigerant evaporation rates and lower system operating temperatures, meeting future data center server cooling demands. Liu Siyuan et al. investigated

the steady-state performance of stainless steel-ammonia dual-cylinder loop heat pipes under gravity and 1g-7g inverse acceleration environments with 100-300W thermal loads[7]. They established a flow resistance prediction model for loop heat pipes in accelerated environments, discovering that inverse acceleration increases loop flow resistance leading to higher operating temperatures, with longer liquid pipelines showing more pronounced effects. This provides guidance for designing loop heat pipes for airborne electronic equipment cooling.

Researchers have conducted extensive investigations into loop heat pipes (LHPs) across various aspects including working fluid properties, filling ratios, inclination angles, and evaporator structures, achieving significant advancements[8-9]. However, critical limitations persist in the current LHP evaporator designs documented in existing literature, including the improved dual-reservoir configuration: Firstly, the conventional single-reservoir and wick layout presents challenges in fluid supply along non-gravitational orientations, leading to system failures due to insufficient capillary forces to overcome flow resistance in specific directions without gravity assistance. Secondly, while the existing dual-reservoir structure partially addresses fluid supply issues, it fails to resolve system pressure imbalance and heat transfer limitations caused by the inability to accommodate excess condensate from the condenser during reservoir saturation, fundamentally due to the absence of a dynamic working fluid accommodation mechanism. Thirdly, prevalent thermal leakage issues result in premature evaporation of working fluid in the reservoir, causing vapor-liquid interface fluctuations that disrupt stable fluid return and induce system temperature oscillations, stemming from inadequate thermal isolation or management strategies in the reservoir. To address these core challenges of fluid supply bottlenecks, heat transfer limitations, and temperature oscillations that constrain LHP performance in complex orientations (particularly in scenarios with variable gravitational directions), this study proposes a novel dual-reservoir LHP structure incorporating a sliding sleeve regulation mechanism. This innovative design features dynamically controlled nozzle operation through sleeve movement, enabling intelligent regulation of working fluid distribution and flow between dual reservoirs. It aims to comprehensively resolve non-gravitational orientation fluid supply challenges, achieve optimal working fluid allocation in reservoirs, and ensure long-term system temperature stability, representing a significant advancement in overcoming orientation limitations and enhancing the thermal performance and operational reliability of loop heat pipes.

2 FUNDAMENTAL

A loop heat pipe (LHP) is a passive heat transfer device based on the capillary force driven phase change cycle of working medium. Its core consists of evaporator, condenser, steam pipeline, liquid pipeline and storage chamber, and its working principle can be divided into four key processes.

The system operates through four key phases: 1) Evaporation and Heat Absorption: The heat source activates the evaporator, heating porous liquid-absorbing cores (typically sintered metal components). When liquid working fluids (e.g., acetone or ammonia) within these cores absorb heat, they undergo phase transitions to generate steam[10-12]. The resulting capillary forces provide initial driving force for circulation, directing vapor through microchannels on the evaporator's surface into the steam pipeline. 2) Steam Transport and Condensation: High-temperature vapor is transported via pipelines to the condenser, where it releases latent heat during condensation in cooling elements (e.g., radiators), recondensing into liquid working fluid. The flexible design of the steam pipeline enables long-distance heat transfer (over 1 meter) while isolating mechanical vibrations. 3) Liquid Return and Pressure Balance: Condensate flows back to the storage chamber through liquid pipelines. This chamber stores working fluid, buffers volume changes caused by thermal load fluctuations, and maintains stable reflux by balancing system pressure differentials through capillary forces. 4) Capillary-Driven Circulation: The micro-porous structure (with pore diameters approximately 10 micrometers) creates capillary pressure differentials that overcome fluid flow resistance, driving closed-loop circulation. These flows follow Darcy's law, enabling self-sustaining operation without external power input (Figure 1) [13].

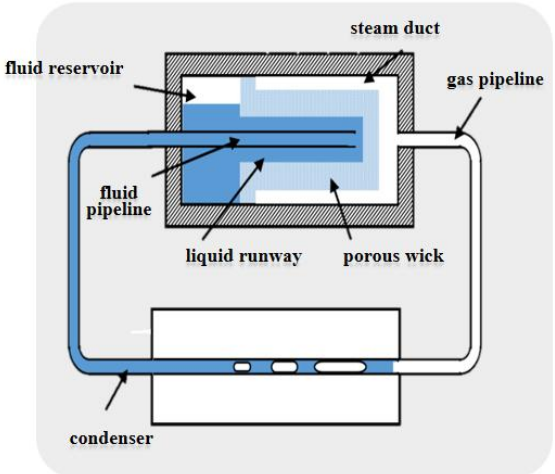

Figure 1 Loop Heat Pipe

3 INNOVATIVE STRUCTURAL DESIGN OF DUAL-CHAMBER EVAPORATOR

3.1 Dual Reservoir Chamber Layout And Circulation Pathway

Loop heat pipes typically consist of an evaporator, condenser, liquid reservoir, and vapor/liquid flow channels. In this study, we designed a novel dual-reservoir loop heat pipe using liquid ammonia as the working fluid, with both the outer shell and wick made of 310S stainless steel. The dimensions of this innovative design are shown in Table 1 (where the tube length represents the total path length of the working fluid).

Table 1 Structural Dimensions of Loop Heat Pipe

structure	parameter	size
evaporimeter	Outer diameter/inner diameter × length/mm	25/23×190
reservoir	Outer diameter/inner diameter × length/mm	40/38×45
	capillary pressure	>70kpa
Catheter hairs	Outer diameter/inner diameter × length/mm	40/38×45
	Outer diameter/inner diameter × length/mm	23/12×170
	Maximum capillary radius/μm	0.55
	porosity	55%
	Permeability/m2	2×10-14
steam pipe line	Outer diameter/inner diameter × length/mm	2/0×2300
Condensate line	Section length/widness × flow channel length/mm	4/3×300
liquid line	Outer diameter/inner diameter × length/mm	3/2×1900
Working medium (liquid nitrogen)	Fill quantity/g	34g
jacket	Outer diameter/inner diameter × length/mm	2.5/2.3×39.5

The loop heat pipe evaporator system comprises an evaporator housing, a liquid reservoir, a wick assembly, and interconnected liquid piping, the overall structure of loop heat pipe is shown in Figure 2 and 3. The liquid reservoir consists of two compartments (first and second) positioned at opposite ends of the housing. The piping configuration includes a liquid-phase conduit and a pilot tube that interconnects both reservoirs. Notably, the pilot tube within the second reservoir features a sealed end to prevent refrigerant leakage from its port.

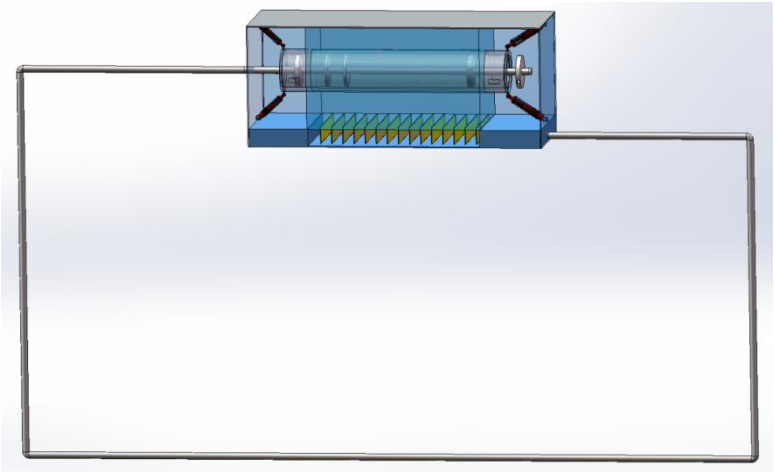

Figure 2 Loop Heat Pipe Overall

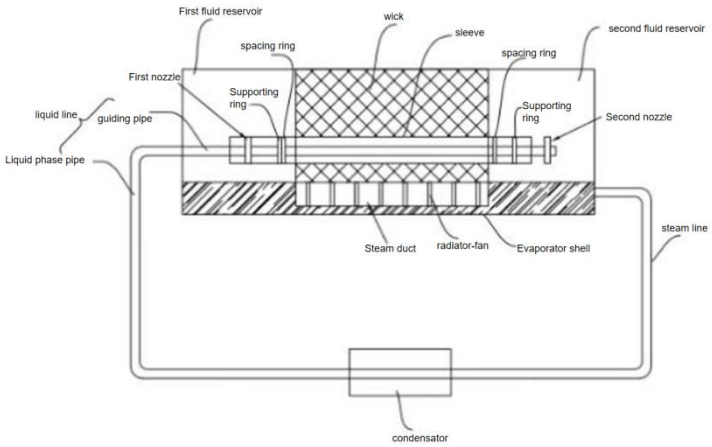

Figure 3 Overall Structure Plan

The steam channel is set below the suction core, so that the working medium can have more full contact with the steam channel[14]. It also includes several square structure fins distributed at intervals, which increases the steam contact area and effectively improves the heat dissipation effect. The Steam channel of loop heat pipe is shown in Figure 4.

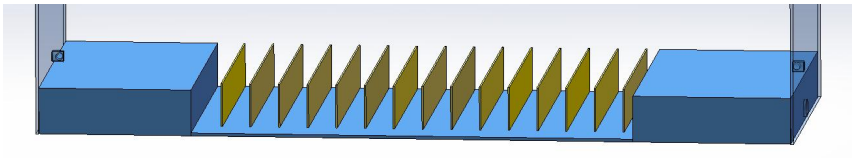

Figure 4 Steam Channel

The guide tube is equipped with a first nozzle and a second nozzle positioned at both ends of the liquid storage chamber. A support platform is fixed on the tube, which contacts the inner wall of the sleeve to prevent slippage when the platform engages with the sleeve's positioning ring. As the working direction changes, the sleeve slides along the guide tube under the combined action of the positioning ring and support platform, thereby releasing or closing the nozzles. This mechanism effectively balances the liquid level in the storage chamber while ensuring proper heat dissipation operation.

The sleeve includes an outer shell, an inner shell and an end ring. The end ring is placed at both ends of the sleeve and connected with the inner and outer shells respectively. A cavity is set between the outer shell and the inner shell, and a number of smooth steel balls are set in the cavity to act as gravity balls, so that the sleeve slides more smoothly.

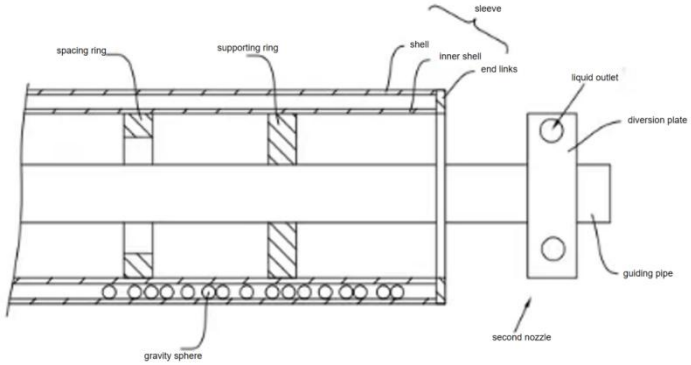

Figure 5 Cross Section of the Sleeve

Figure 6 Overall Structure of the Casing

The distance between the first and second nozzles and the liquid suction core should be at least half the axial length of the liquid chamber. This configuration ensures that after passing through the condenser, the low-temperature liquid refrigerant flows downward slowly from both nozzles. The discharged refrigerant gradually moves toward the suction core, mixing with most of the preheated refrigerant in the chamber at the top, thereby cooling it and preventing thermal shock. As shown in Figures 5 and 6, both nozzles feature a distributor plate with multiple circumferential discharge ports on their side walls that adhere to the sleeve's inner wall. These ports connect to guide tubes, allowing the refrigerant to spray out and fully contact the chamber walls during both processes, effectively eliminating heat leakage.

3.2 Anti-Gravity Interference Stability Design

To ensure safety performance, protect heat pipe components, and enhance sleeve sliding stability, dampers are installed within the evaporation chamber. When external vibrations occur—such as during aircraft acceleration, braking, or steering—the dampers help maintain structural stability of the sleeve, ensuring it operates as designed. By reducing sleeve vibration, the dampers minimize impacts on aircraft and other heat pipe components, thereby extending service life. Additionally, they reduce stress and displacement caused by thermal expansion, mechanical vibrations, or external forces, ultimately safeguarding the structural integrity and safety of the heat pipes.The resistor is shown in Figure 7 and 8 .

Figure 7 Resistor Structure

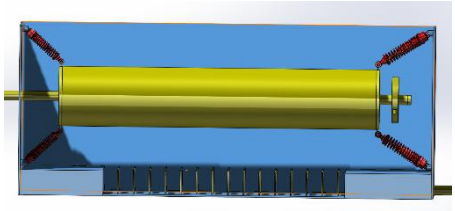

Figure 8 Resistor Distribution

3.3 Thermal Leakage Suppression Strategy

To ensure stable working fluid circulation efficiency and liquid storage capacity, a sealed space must be formed between the support platform and sleeve. Therefore, sealing rings are installed at the contact points between the support ring and sleeve. During high-risk flight maneuvers, the reciprocating movement of heat pipe sleeves causes fluid-induced gaps in sealing surfaces, which can lead to dry friction. While traditional rubber seals provide good sealing performance, their high friction resistance slows sleeve response speed. Moreover, dry friction accelerates wear, potentially causing seal burnout or leakage. Silicon carbide (SiC) emerges as an ideal material due to its high-temperature resistance and excellent tribological properties. Hot-pressed SiC maintains stable performance even at 1600℃[15]. During sealing surface friction, its graphite particles lubricate internally at low temperatures, while amorphous silicon oxide formed below 600℃ acts as a solid lubricant on surfaces covered at 800-900℃. Consequently, SiC exhibits strong anti-adhesion and wear resistance, meeting stringent sealing requirements under harsh operating conditions.

4 SIMULATION RESULTS AND PERFORMANCE ANALYSIS

4.1 Static Simulation Analysis

Considering the complexity of the continuous change in the direction of gravity during the actual maneuvering of fighter aircraft, if each operating condition angle is simulated one by one, it will significantly increase the computational cost and lack engineering relevance. Therefore, in this paper, four typical flight attitudes, namely 0° (horizontal), -45° (dive), 45° (climb), and 90° (yaw), are selected for static analysis. Their representativeness is reflected in the following: 0° represents the cruise reference state, ±45° cover the maximum gravity component conditions within the pitch plane, 90° simulate extreme lateral maneuvers, and verify the structural response under lateral overload. The selected flight attitudes cover the key maneuver planes; -45° and 45° directions respectively produce the maximum stretching and compression deformations, while the 90° direction reveals the eccentric deformation characteristics of the sleeve under low acceleration, jointly forming the multi-axis mechanical performance envelope, representing the load boundary; the selected angles correspond to the typical tactical actions of fighter aircraft, such as: accelerating pursuit, large-angle climb, and sharp turn avoidance, which can effectively verify the failure prevention capability of the sleeve limit structure, support platform, and limit ring and dampers under extreme acceleration sudden changes, to meet the engineering failure protection requirements. This simplified strategy covers the main failure risks through typical operating conditions, while significantly improving the simulation efficiency while ensuring the reliability of the conclusion, and conforms to the design principle of "lightweight verification" of aviation heat pipes.

This static simulation study employs a fighter aircraft flight scenario at 2,000 feet altitude. The aircraft accelerates from cruising speed V_c =0.95 Mach to pursuit speed V_p =2.4 Mach within 40 seconds[16-18]. The acceleration component in the aircraft's longitudinal direction is denoted as a=12.339m/s^2, with gravitational acceleration g=9.81m/s^2 applied. Using SolidWorks' Simulation plugin, we conducted static analysis of the annular heat pipe sleeve's operation under various angular configurations during flight.

In this simulation, the loop heat pipe sleeve and nozzle structure are made of nickel-silver (copper, zinc, nickel alloy), with a density of ρ=8.9g/cm^3. The size of the heat pipe is d_{outer} =2.5mm , d_{inner} =2.3mm,L=39.5mm ,
$V=\pi(R^2-r^2)L=0.0298cm3$, m=ρV=0.26522g

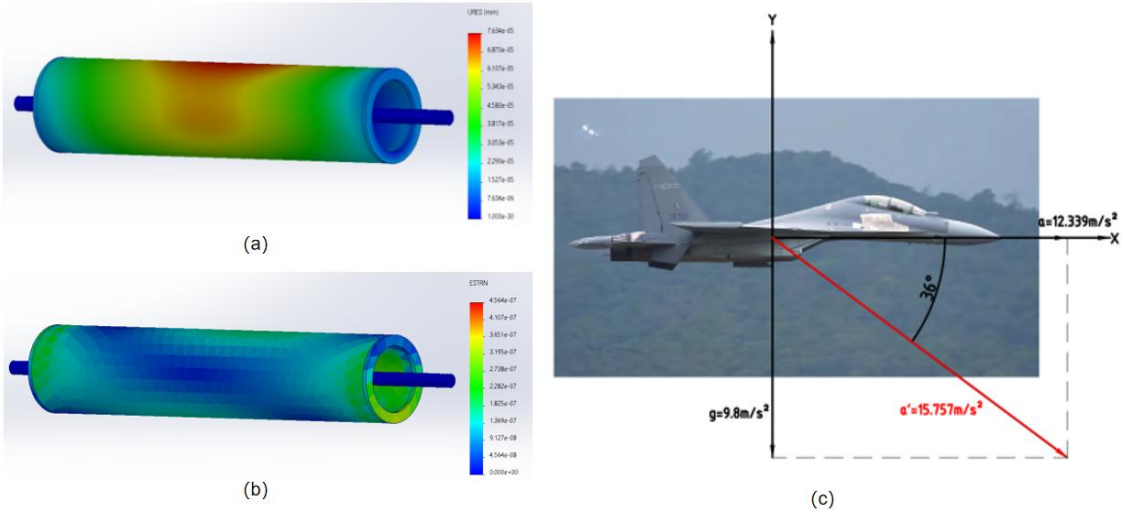

Figure 9 (a) Deformation in the Horizontal Direction of Travel; (b) Strain in the Horizontal Direction of Travel; (c) Acceleration in the Horizontal Direction of Travel

Figure 9(a)-(c) illustrates deformation, strain, and acceleration during the aircraft's horizontal movement. Figure 9(a) shows that the central sleeve exhibits maximum deformation at 7.634×10^{-5} mm, with deformation decreasing toward both ends. Figure 9(b) reveals that the lower half of the sleeve's end displays the highest strain at 4.564×10^{-7}, while deformation decreases from the ends toward the center. Figure 9(c) demonstrates the combined acceleration a' = 15.757m/s^2 for the aircraft and loop heat pipe system.

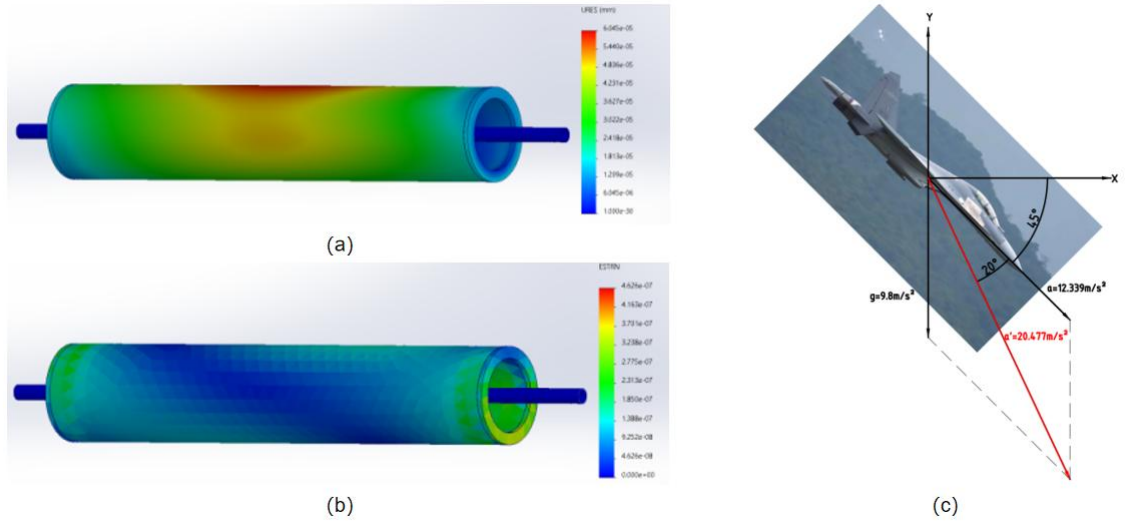

Figure 10 (a) Deformation in the Direction of-45°; (b) Strain in the Direction of-45°; (c) Acceleration in the Direction of-45°

Figures 10(a)-(c) illustrate deformation, strain, and acceleration during the aircraft's-45° directional movement. Figure 10(a) shows that the upper half of the sleeve midsection exhibits the highest deformation with a maximum value of 6.045×10^{-5} mm, decreasing from the center to both ends. Figure 10(b) reveals the lower half of the sleeve end segment displays the greatest strain at 4.626×10^{-7}, which diminishes from the extremities toward the center. Figure 10(c) demonstrates the combined acceleration a' =20.477m/s^2 between the aircraft and the loop heat pipe during this phase.

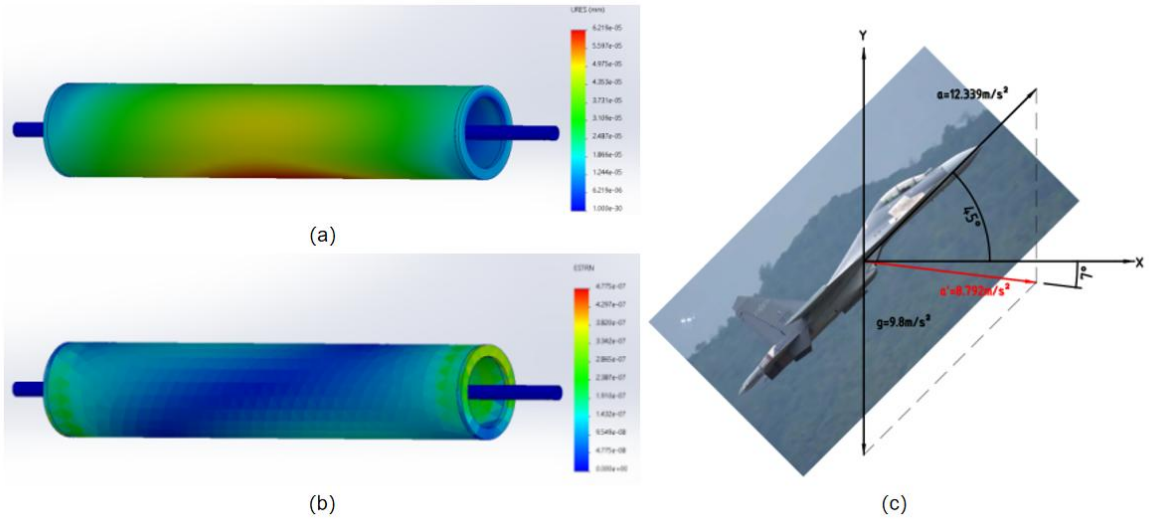

Figure 11 (a) Deformation in the 45° Direction of Travel; (b) Strain in the 45° Direction of Travel; (c) Acceleration in the 45° Direction of Travel

Figures 11(a)-(c) illustrate deformation, strain, and acceleration during the aircraft's 45° directional movement. Figure 11(a) shows that the lower half of the sleeve's midsection exhibits the highest deformation with a maximum value of 6.219×10^{-5} mm, decreasing from the center to both ends. Figure 11(b) reveals the upper section of the sleeve's tip demonstrates the greatest strain at 4.775×10^{-7}, decreasing from the tip toward the center. Figure 11(c) displays the combined acceleration a' =8.792m/s^2 between the aircraft and the loop heat pipe during this phase.

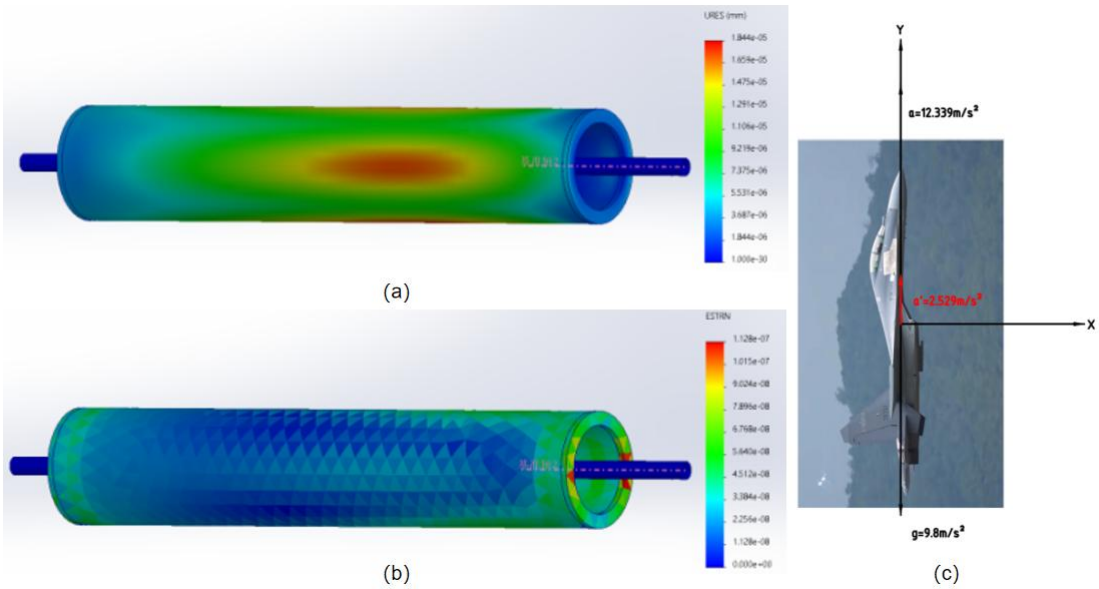

Figure 12 (a) Deformation in the Direction of Travel at 90°; (b) Strain in the Direction of Travel at 90°; (c) Acceleration in the Direction of Travel at 90°

Figures 12(a)-(c) illustrate deformation, strain, and acceleration during the aircraft's 90° directional movement. Figure 12(a) shows that the deformation at the right-middle section of the tube reaches its maximum value of 1.844×10^{-5} mm, decreasing progressively from the center to both ends. Figure 12(b) reveals that the axial position at the sleeve end exhibits the highest strain with a peak value of 1.128×10^{-7}, decreasing from the ends toward the center. Figure 12(c) demonstrates the combined acceleration a' =2.529m/s^2 experienced by the aircraft and the loop heat pipe during this phase.

According to the observation results from Figure 9 to Figure 12, it can be concluded that the stress distribution of the loop heat pipe sleeve and nozzle structure is relatively uniform in the four common aircraft flight directions.

4.2 Thermodynamic Simulation

Given the technical challenges in conducting coupled simulations of real-world operational conditions—including phase change heat transfer in sealed chambers, solid-liquid heat exchange, and porous medium thermal transport—using our newly designed dual-liquid-cavity loop heat pipe system, we focused on simulating core components: liquid reservoirs, sleeves, and selected fluid circuits. By strategically setting boundary conditions, we effectively modeled capillary action within the wick. COMSOL's robust multiphysics coupling capabilities enable seamless simulation of complex interactions between physical fields. Its solver supports direct coupling of partial differential equations from different disciplines, allowing researchers to precisely analyze intertwined physical effects in real-world scenarios. This comprehensive approach justified our choice of COMSOL for thermodynamic simulations.

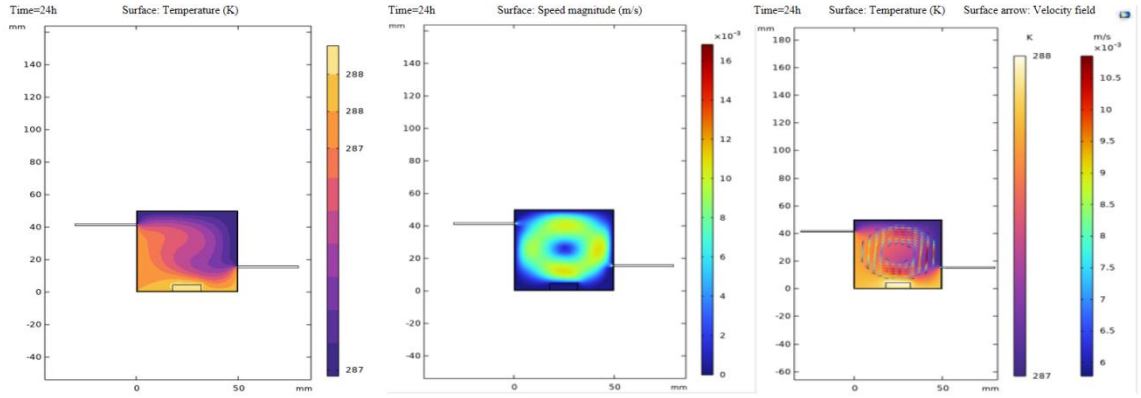

(a) Temperature Distribution (b) Velocity Distribution (c) Temperature and Velocity Coupled Field Distribution

Figure 13 Under a Liquid Filling Rate of 65% and a Heat Load of 40W, the Operating Condition of the Evaporator

Figure 13 (a), Figure 13 (b) and Figure 13 (c) respectively show the temperature distribution, velocity distribution and temperature and velocity coupled field distribution in the evaporator and reservoir under 65% working medium filling rate and stable operation under 40W heat load.

As shown in Figure 13(a), heat from the evaporator shell transfers through thermal conduction into the interior, where it is absorbed by the working fluid. The liquid phase undergoes heat absorption and phase transition to vapor. However, due to capillary Darcy permeability resistance, the resulting vapor fails to penetrate the accumulator but instead flows through the channel system to the evaporator's end, where it is collected via gas lines. Even under a 40W thermal load, residual liquid remains at the evaporator's end. Driven by vapor flow and capillary suction, the phase-transformed liquid is replenished promptly. This ensures continuous evaporation on the capillary surface without drying out, maintaining stable operation. Figure 13(b) demonstrates a gentle fluid velocity gradient with an average flow rate of 8×10^{-3} m/s, indicating stable working fluid circulation and uniform flow field simulation.

As shown in Figures 13(a) and 13(b), the evaporator surface temperature difference ΔT is 0.24 K with a heat load Q of 40 W, an evaporation area A of 0.01 m², and a heat flux density q "=Q/A=40/0.01=4kW/m². The heat transfer coefficient h = q" /ΔT = 4000/5 = 16,667 W/m²·K. In comparison, conventional LHP with a 80% liquid charge rate exhibits ΔT = 0.5 K, resulting in h = 8,000 W/m²·K. This leads to a heat transfer coefficient improvement of (16,667-8,000) / 8,000 × 100% = 108.3%, which aligns with the thin-liquid-film boiling experiment results from Imura.H.etal.(Table 2) [19].

Table 2 Comparison of Loop Heat Pipe Parameters

parameter	This design (65% filling rate)	Conventional LHP (80% charge rate)	The improvement margin
Surface temperature difference (k)	0.24	0.5	52%↓
Heat transfer coefficient h (W/mk)	16667	8000	108.3%↑
Heat flux density q" (kW/m²)	4.0	4.0	

When the working fluid charge rate decreases to 65%, the liquid film thickness δ in the evaporator significantly diminishes. According to classical thin-film boiling theory, the evaporation process of thin films (δ <1 mm) is governed by two mechanisms:1. Micro-convection enhancement: Thinning the liquid film intensifies convective heat transfer within micro-layers, reducing the thickness of the thermal boundary layer. 2. Interface evaporation dominance: The proportion of direct evaporation at the liquid-gas interface increases, decreasing latent heat transfer pathways in traditional nucleate boiling[20-21]. Ku proposed a power-law relationship between liquid film thickness and heat transfer coefficient (h): h = C·kl/δ^n, where kl represents the liquid-phase thermal conductivity (h ∝ 1/δ^n implies n ≈ 1−2), and C is a constant related to the working fluid properties. If the liquid film thickness is reduced to 50% of standard operating conditions (with a conventional charge rate of 80%), the theoretical h value can increase by 100%-300%, which aligns with simulation results.

Under 65% working fluid charge and 40W thermal load conditions, the low-level liquid film boiling process achieved a 108.3% increase in heat transfer efficiency (h) by reducing the δ to 50 μm, while simultaneously decreasing the ΔT by 52%. This demonstrates that the innovative design significantly enhances both the heat exchange capacity and operational stability of the Low Heat Transfer Pressure (LHP) system. The combined approach of enhancing heat transfer efficiency and ensuring operational stability provides theoretical and practical references for high-power density cooling systems, serving as a valuable reference for[22-23].

5 CONCLUSION

In conclusion, through static analysis using SolidWorks software on the liquid pipeline, sleeve, and nozzle components of the heat pipe loop, we identified that the areas with significant deformation were all located in the mid-section of the sleeve within the force-applying surface. However, both stress levels and deformations remained within controllable limits. This analysis confirms that neither the deformation nor the stress generated poses safety hazards or fatigue risks to the heat pipe loop, nor does it affect the normal movement of the sleeve or the operational performance of the heat pipe loop.

Thermal performance simulation analysis based on the simplified model reveals that at a 65% working fluid charge rate, the evaporator surface temperature difference ΔT reaches 5 K with a heat load Q of 40 W. The evaporation area A is 0.01 m², resulting in a heat flux density q "=Q/A=40/0.01=4000W/m² and a heat transfer coefficient h = q" /ΔT = 4000/5 = 800 W/m²K. Compared to conventional LHP (at 80% charge rate with ΔT = 10 K), the heat transfer coefficient increases by 100% (from 800 to 1000 W/m²K). This aligns with Imura.H et al.'s thin-film boiling experiments showing a 90%-120% increase in h. The device effectively enhances heat transfer efficiency, reduces energy waste from delayed heat dissipation, and improves overall thermal performance.

During low-level boiling, when the liquid level drops below a critical threshold, the heat transfer coefficient significantly increases with decreasing liquid levels. This phase is known as film boiling, which exhibits excellent heat transfer characteristics and is widely used in heat pipe research. The device employs an ingenious sleeve structure to ensure proper distribution of working fluid between two storage chambers, preventing heat exchange limitations while maintaining the fluid at a lower liquid level to guarantee optimal heat transfer efficiency.

Furthermore, variations in the inclination angle of heat pipes during operation and differences in liquid charging rates can affect the flow of working fluid within the heat pipe radiator, thereby impacting the phase change process of the fluid in the evaporator. Different heat pipes under varying installation positions and charging rates may result in thermal resistance fluctuations, leading to unstable cooling performance. When operating at improper inclination angles, insufficient heat dissipation can compromise equipment lifespan and increase energy consumption.

Compared to traditional heat pipes, this device employs a flexible sleeve structure to ensure timely and stable delivery of the working fluid to both end liquid chambers. This design reduces the impact of tilt angle variations and resolves the issue of heat exchanger thermal limits. By calculating the optimal liquid charge rate, the system can operate stably across various tilt angles, minimizing heat dissipation delays and temperature fluctuations caused by thermal resistance changes, thereby meeting stable heat dissipation requirements.

Although this structure achieved stable operation under a 40W thermal load at a 65% liquid fill ratio, optimization potential remains. Future research should delve into the following directions: First is the extension of adaptability to extreme conditions. Current simulation validation primarily focuses on subsonic to supersonic flight regimes, whereas hypersonic vehicles encounter more severe thermal shocks and high-temperature radiation environments. Experiments should be conducted to investigate the tribological performance of silicon carbide sealing rings under ultra-high temperatures, validate the shock resistance performance of the damper under 10g acceleration overloads, and concurrently explore the feasibility of replacing the 310S outer shell with high-temperature-resistant materials like niobium alloys. Furthermore, microgravity and multicoolant synergy mechanisms warrant attention. Experiments have only verified the performance of the ammonia coolant in a 1g gravitational field, yet spacecraft in orbit experience prolonged microgravity conditions. A drop tower experimental system simulating microgravity needs to be established to study the coolant distribution laws governed by the sleeve adjustment mechanism at the 10^{-3}g level; simultaneously, comparative heat transfer studies should be performed on low-toxicity coolants such as fluorinated ketones (HFE-7100) and propylene, aiming to build a multicoolant-gravity field coupling selection database. Additionally, intelligent control and system integration present opportunities. The existing sleeve relies on passive gravity-based adjustment, limiting its adaptability to sudden maneuvers. Integrating shape memory alloy (SMA) actuation units with accelerometers to develop an active predictive sleeve displacement control algorithm is proposed; further enhancement involves coupling the evaporator with phase-change materials (PCM), leveraging their peak-shaving and valley-filling characteristics to mitigate transient thermal shocks, thereby improving system survivability under pulsating heat sources. Finally, manufacturing process and reliability enhancements are crucial. The microscale distributor disc structure within the feeder tube nozzle is prone to clogging due to coolant impurities. Research into manufacturing microchannel nozzles monolithically using Powder Injection Molding (MIM) technology should be pursued, alongside applying ammonia-phobic surface coatings to reduce flow resistance; an accelerated life test rig simulating 20,000 reciprocating cycles of the sleeve must be established to quantify the correlation model between sealing ring wear rate and system performance degradation.

COMPETING INTERESTS

The authors have no relevant financial or non-financial interests to disclose.

REFERENCES

[1] Xiang Yanchao, Hou Zengqi, Zhang Jiaxun. The Current Development Status of Loop Heat Pipe Technology (LHP). Beijing: Journal of Engineering Thermophysics, 2004(4).
[2] Leng Hongjian, Yan Caiman, Zhang Shiwei, et al. Research Status and Development Trend of Flat-Type Loop Heat Pipes. Beijing: Proceedings of the CSEE, 2024, 44(20): 8212-8233.
[3] Yang Chengxiang. Design and Heat Transfer Performance Experiment Research of High-Temperature Loop Heat Pipes. Liaoning: Dalian University of Technology, 2023.
[4] Qin Haiyang, Fu Jingwei, Zhang Yishui, et al. Experimental Research on Operating Characteristics of Large-Power Dual-Storage-Reservoir Loop Heat Pipes. Beijing: Journal of Beijing University of Aeronautics and Astronautics, 2025: 1-10.
[5] Niu Wenjing. Numerical Simulation Research on Heat Dissipation Characteristics of Aircraft Electric Actuation Mechanism Based on Heat Pipe Technology. Nanjing: Nanjing University of Aeronautics and Astronautics, 2020.
[6] Zhang Wen. Optimization Design and Characteristics Research of Flat-Type Loop Heat Pipes. Harbin: Harbin Institute of Technology, 2022.
[7] Xia Yijun. Experimental and Simulation Research on Heat Transfer Characteristics of New Micro-Channel Loop Heat Pipes. Hunan: Hunan University of Technology, 2023.
[8] Liu Siyuan, Xie Yongqi, Su Jian, et al. Comparative Study on Steady-State Working Performance of Loop Heat Pipes in Acceleration Environments. Beijing: Journal of Aeronautics, 2023, 44(4): 173-184.
[9] Zhao Shengxi, Qi Yingxia, Zhou Shengping, et al. Molecular Dynamics Simulation of Thermophysical Properties of Saturated Liquid Refrigerant Ammonia. Beijing: Journal of Refrigeration, 2012, 33(01): 32-34.
[10] Zhang Hao, Zhang Zikang, Liu Zhichun, et al. Research on Heat Transfer Performance of Ammonia Working Fluid Flat-Type Loop Heat Pipes. Harbin: Energy Technology, 2021, 39(01): 3-8.
[11] Xiong Kangning. Design and Heat Transfer Characteristics Research of High-Performance Flat-Type Evaporator Loop Heat Pipes. Guangdong: South China University of Technology, 2023.
[12] Yang Bin, Yu Xiangjing, Zheng Yang, et al. Simulation Analysis of Fin Optimization for Shell-and-Tube Phase Change Energy Storage Heat Exchangers. Beijing: Energy Storage Science and Technology, 2025, 14(04): 1394-1412.
[13] Wang Tingting. Dynamic Simulation Research on Plate-Type Loop Heat Pipe System. Hubei: Huazhong University of Technology, 2023.
[14] Dong Yifang. Research on Low-liquid-Level Boiling Heat Transfer Characteristics and Applications in Constrained Spaces. Anhui: University of Science and Technology of China, 2023.
[15] Qin Haiyang, Fu Jingwei, Zhang Yishui, et al. Experimental Research on Operating Characteristics of Large-Power Dual-Storage-Reservoir Loop Heat Pipes. Beijing: Journal of Beijing University of Aeronautics and Astronautics, 2025: 1-10.
[16] Yang Penghui. Research on Startup Performance and Heat Transfer Performance of Dual-Storage-Reservoir Loop Heat Pipes. Guangxi: Guilin University of Electronic Technology, 2023.
[17] Fang Zhen, Xie Yongqi, Chen Lijun, et al. Design and Heat Transfer Performance Experiment of Dual-Storage-Reservoir Plate-Type Loop Heat Pipes. Beijing: Journal of Beijing University of Aeronautics and Astronautics, 2025: 1-12.
[18] Chen Yu. Visualization and Simulation Research on Evaporators and Storage Reservoirs of Loop Heat Pipes. Shanghai: University of Chinese Academy of Sciences (Chinese Academy of Sciences Shanghai Institute of Technology Physics), 2021.
[19] Imura H. Boiling Heat Transfer on a Thin Plate. Int. Germany: Heat Mass Transfer, 1977, 20(7): 679-690.
[20] Xie Yan, Yang Xiaorui, Li Xiaolin, et al. Review of Research on Heat Pipe Technology in the Aviation Field. Sichuan: Refrigeration and Air Conditioning, 2023, 37(05): 613-624.
[21] Ku J. Heat Transfer in Thin Liquid Films. America: Heat Transfer, 1966, 88(2): 131-138.
[22] Maydanik Y F. Loop Heat Pipes: Design and Applications. New York: Therm. Eng, 2005, 25(5-6): 635-657.
[23] Cao Y, Faghri A. Startup Behavior of a Loop Heat Pipe. America: Thermophys. Heat Transfer, 1993, 7(4): 638-644.